SYNTHESIS AND CHARACTERISATION OF NOVEL HALLOYSITE NANOTUBES/CHITOSAN COMPOSITE MEMBRANES

R. T. De Silva [1], P. Pasbakhsh[1*], G. K. Lim[2], and C. S. Piao[1]

[1] *Department of Mechanical Engineering, School of Engineering, Monash University Sunway Campus (MUSC), 46150, Sunway, Malaysia.*

[2] *School of Mechanical and Systems Engineering, Newcastle University, Singapore*
**e-mail address of the corresponding author: Pooria.pasbakhsh@monash.edu.*

Keywords: Chitosan, Halloysite Nanotubes, Solution Casting.

Abstract
Novel membranes of chitosan/Halloysite Nanotubes (HNTs) nanocomposites were prepared using solution casting method by adding 2 wt%, 5 wt%, 10 wt% and 15 wt% of HNTs. Mechanical properties, such as Young's modulus and tensile strength of nanocomposites at 5w% of HNTs significantly improved by 21% and 34%, respectively, compared to unreinforced chitosan membranes. At high HNT concentrations mechanical properties were slightly inferior to the chitosan membranes with 5 wt% of HNTs, due to the aggregation of HNTs. Scanning electron microscopy (SEM) of membranes at 2 % and 5 wt% of HNTs showed low amounts of pulled-out nanotubes which confirmed the presence of more embedded nanotubes inside the chitosan matrix as well as less amounts of micro-voids at the fractured surface of chitosan/HNTs nanocomposites. FTIR shows possible interaction of external surface siloxane groups of the HNTs with the matrix. Thermal Gravimetric Analysis (TGA) revealed that thermal stability of nanocomposites increased by increasing the HNTs concentrations.

1 Introduction

Chitosan, 'poly-b (1,4)-2-amino-2-deoxy-D-glucose', is a deacetylated product of chitin which may be derived from crab, shrimp shells and fungal mycelia [1]. Owing to its non-toxic nature, antimicrobial activity, and good compatibility with living tissues chitosan has been identified as a good candidate for use as a biomaterial during the last 20 years [2]. The most convenient methods for chitosan production are melt-blending and solution casting [3]. From structure-function point of view, of the many varied forms, chitosan membrane is the most versatile particularly for biomedical applications such as tissue engineering, bone implantation and artificial skin [3-5], as well as for water filtration applications such as waste water filtration and reverse osmosis [6].

However, chitosan has low mechanical strength, thermal stability, water and gas barrier properties, which restrict the opportunity for wider applicability [2, 7]. Different types of micro and nanofillers such as silica particles, hydroxyapatite, calcium phosphate cement,

carbon nanotubes (CNTs) [8] and organo modified montomorillonite (OMMT) crystallites have been studied for reinforcing chitosan [9]. However, it is well known that the synthesis and functionalization processes of all these fillers are complicated and costly [10].

Halloysite nanotubes (HNTs) are natural aluminosilicate ($Al_2Si_2O_5(OH)_{4.n}H_2O$) crystallites with nano-tubular structures [10]. Typically, the length of HNTs varies from 50-5000 nm, with an external diameter of 20-200 nm and internal diameter of 10-70nm [11]. HNTs possess several remarkable properties such as biodegradability, low surface hydroxyl groups and unique crystalline structure. Consequently, beside drug delivery and anticorrosion HNTs have been used as nanofillers to reinforce various polymers [12]. Dobrovol'skaya et al. (2011) have explored the physical properties of chitosan fibers containing chrysotile and HNTs; they have observed that adding HNTs increases the mechanical properties of chitosan fibers [13].

In this study synthesis and characterization of chitosan-HNT membranes have been studied. A solution-casting approach has been developed and implemented for fabricating the membranes.

2. Materials and testing Methods

Chitosan of low molecular weight with an 85% degree of deacetylation, was purchased from Sigma Aldrich. HNTs from New Zealand were provided by Imerys Tableware Asia Limited, New Zealand. One gram of chitosan was mixed in 100 ml of 1% acetic acid solution and stirred for 20 h. Next distilled water was mixed with 2, 5, 10 and 15 (w/w %) of HNTs with respect to 1 g of chitosan. Following this, the mixtures were placed in an ultrasonic bath (*Thermo D-60)* for 30 min at a temperature of 50°C. Thereafter, the mixture was stirred for 20 h. Next, the solutions of chitosan and HNT were mixed together and stirred. Following this, 15 g from the resultant respective solutions was poured into plastic petri dishes. To ensure that the solution precipitates into a membrane, the dishes were placed in an oven for 20 h at 40°C. After membrane formation, each dish was filled with sodium hydroxide (30 ml, 0.1 M) and left for 30 min to neutralize any left-over acetic acid. Following this, the membranes were submerged in distilled water for 30 min to remove the sodium hydroxide. Finally, the membranes were peeled off from the plastic dishes.

A high-throughput small-scale horizontal tensile test rig was used to determine the tensile properties of the membrane with a specimen size of 3 mm×150 mm at a 0.06 mm/s. Young's modulus (E), tensile stress (σ) and elongation at break (E_b) reported here represent average results for at least 10 specimens. In order to measure the tensile properties of prepared membranes were cut into 3mm x 15mm rectangular pieces and pasted on the paper template. Cross section areas of the tensile specimens were determined using an Olympus BU41optical microscope.

The fractured surfaces of tensile samples with 2, 5 and 15 (w/w %) of HNTs were investigated by using a *Supra-35VP SEM*. To prevent electrostatic charging during observation, the samples were coated with a thin layer of platinum.

FTIR analysis was conducted to identify the chemical interactions occurring inside the nanocomposite membranes and the consistency of the samples. All samples were examined using the *Thermo Scientific IS10* with a wave length range of 400-4000 cm^{-1} with 0.2 cm^{-1} resolution.

TGA was carried out using *TGA Q50* to investigate the thermal stability of the chitosan/HNT nanocomposite membrane, from a temperature range of 25˚C to 600˚C at a rate of 10˚C/min under nitrogen atmosphere.

3.0 Results and Discussion

3.1 Mechanical Properties

The Young's modulus (E), tensile strength (TS) and elongation at break results are summarized in Table 1. Mechanical properties such as E and TS of chitosan membranes have increased with the addition of HNTs. This could be due to the good interaction between the HNTs and chitosan at low HNT concentration. Both E and TS have increased with the addition of 2 and 5 (w/w %) of HNTs. However, E and TS gradually decreased at higher concentrations of HNTs, 10 and 15 (w/w %). In general, E behaves according to the *mixture of law*, which has been explained by a linear equation. But the results of this experiment (trend) shows that the E of the membranes does not follow a linear relationship with the addition of HNTs, and it was clarified using linear regression analysis. At high HNT concentrations, there is a high probability for HNTs to interact with each other and become aggregated. These aggregations formed clusters inside the matrix which led to high stress concentration areas within nanocomposite. Hence, the material failed easily, it can be concluded that the chitosan membranes with 10 (w/w %) and 15 (w/w %) of HNTs may have more clusters of HNTs than the membranes with 5 (w/w %). This has led to the decreasing trend of E after reaching a maximum at 5 (w/w %). Due to the aggregation of HNTs within the matrix at higher concentrations, the E decreased slightly, but it is almost stable, with further increases in the HNT content. For instance, at 10 (w/w %) and 15 (w/w %) of HNTs, E of the chitosan/HNT membrane is 0.503 GPa and 0.505 GPa, respectively, which is only a 0.002 GPa difference. This finding suggested that the E of the nanocomposites is determined by the volume fraction of HNTs and is affected by their distribution and aggregation.

HNT concentration (w/w %)	Young's Modulus (GPa)	Tensile Stress (MPa)	Elongation at break, E_b %
0	0.433±0.017	60.76±2.78	33.6±1.3
2	0.507±0.020	71.20±4.20	22.7±1.2
5	0.522±0.011	81.62±4.36	29.7±2.2
10	0.503±0.018	71.90±3.69	26.7±2.5
15	0.505±0.023	70.93±2.92	23.3±2.5

Table 1: Mechanical properties of chitosan nanocomposite membranes with different HNT compositions.

According to Wang et al. (2005), a reinforcement effect from the finely dispersed nano-fillers throughout the biopolymer matrix also leads to a better mechanical properties [8]. The tensile strength of a material depends on the weakest fracture path throughout the material. In case of nanocomposite materials, hard particles (which could be formed by agglomeration of nanoparticles as well) affect the TS in two ways. One is the weakening effect due to the stress concentration caused by hard particles, while the other is the reinforcing effect as they may serve as barriers to crack growth [14]. Hence it can be concluded that the chitosan membranes

with 5(w/w %) of HNTs have substantially better dispersion than other HNT compositions since it has the highest TS value. It is believed that chitosan membranes with 10 (w/w %) and 15 (w/w %) of HNTs could not have better dispersion of HNTs and consisted of more HNT aggregates. Since there are HNT clusters in high HNT concentration, stress concentration is high and this could be the reason why 10 (w/w %) and 15 (w/w %) membranes have less TS compared to 5(w/w %) However it should be noted that this TS value is still higher than TS of pure chitosan membranes.

Theoretically, E_b decreases when the composite becomes stiffer. In this case, it can be noted that the E_b of chitosan membranes with various HNT concentrations is less than the control sample and E_b followed a decreasing trend from 0 to 15 (w/w %) of HNTs, although E_b has slightly increased up to 29.7% with the addition of 5 (w/w %) . This means that E_b of membranes with different HNT concentrations are not showing any consistent trend in this study. This could be occurring due to the poor dispersion of HNTs at high concentrations and the dominant effect of HNT-HNT interactions at high concentrations. Many researchers have observed discrepancies in the behavior of the E_b in different composite membranes. For example, Hong et al. (2010) observed that E_b of a chitosan/montmorillonite nanocomposite membrane with different montmorrilonite concentration were not even and did not show any consistent trend [2]. Generally, it can be explained that E_b decreased for all nancomposite membranes with respect to the control sample due to the enhanced rigidity of the chitosan chain, resulting from the restriction effect of HNTs [7].

3.2 Morphology

The SEM morphology of the tensile fractured surfaces of the chitosan membranes with 2, 5, and 15 (w/w %) of HNTs are shown in Figure 1. The light circular dots shown in the micrographs are believed to be the end of the tubes. Hence, it can be seen that chitosan membranes with 2 and 5 (w/w %) of HNTs have better dispersion than the membranes with15 (w/w %). Additionally, embedded HNTs in chitosan matrix can be seen in the micrographs. These embedded HNTs confirm the good interaction between the HNT and the matrix. Furthermore, micro-voids can be noticed in the fractured surfaces (marked by arrows) due to the pulled out HNTs during the tensile testing. Pores can also be seen due to the pulled out tubes from matrix during the tension. The presence of agglomerated HNTs was also observed, as circled in Figure 1c. This could be two or more HNTs stacked together in both places, and referred to as HNT aggregated areas. In membrane with 15% HNTs, only few HNT-HNT interactions were spotted and it is believed that many HNT aggregated areas exist and are covered with chitosan in this sample. Difficulty to spot individual tubes in the matrix due to presence of many embedded halloysite in the matrix led to conclude that there was a good interaction between chitosan matrix and tubes in the membranes with all compositions. Nevertheless, filler-matrix interaction of chitosan membranes at low HNT concentrations (2 and 5 (w/w %)) had better dispersion than the high concentrations. Furthermore, it can be observed that low concentrations had less micro-voids and pores compared to high HNT concentration membranes, and these findings suggested that the filler-matrix interaction was strong in those particular concentrations. Even though the morphology and dispersion for the membranes with 2 and 5 (w/w %) were almost similar, the membranes with 5 (w/w %) HNTs has more HNTs which allow for better stress transformation than the 2 (w/w %) HNTs membranes. This is why membranes with 5 (w/w %) of HNTs have high mechanical properties among the other compositions.

The chitosan membrane with 15 (w/w %) of HNTs has more micro-voids, embossed HNTs, and pores. Hence, it can be concluded that chitosan membranes with high HNT concentration do not have better filler-matrix interaction compared to low HNT concentration membranes. According to the tensile test results, mechanical properties such as E and TS of 15 (w/w %) membranes are less than the 5 (w/w %) HNTs membranes. The 15 (w/w %) membranes are also slightly inferior to the membranes with 2 w% of HNTs.

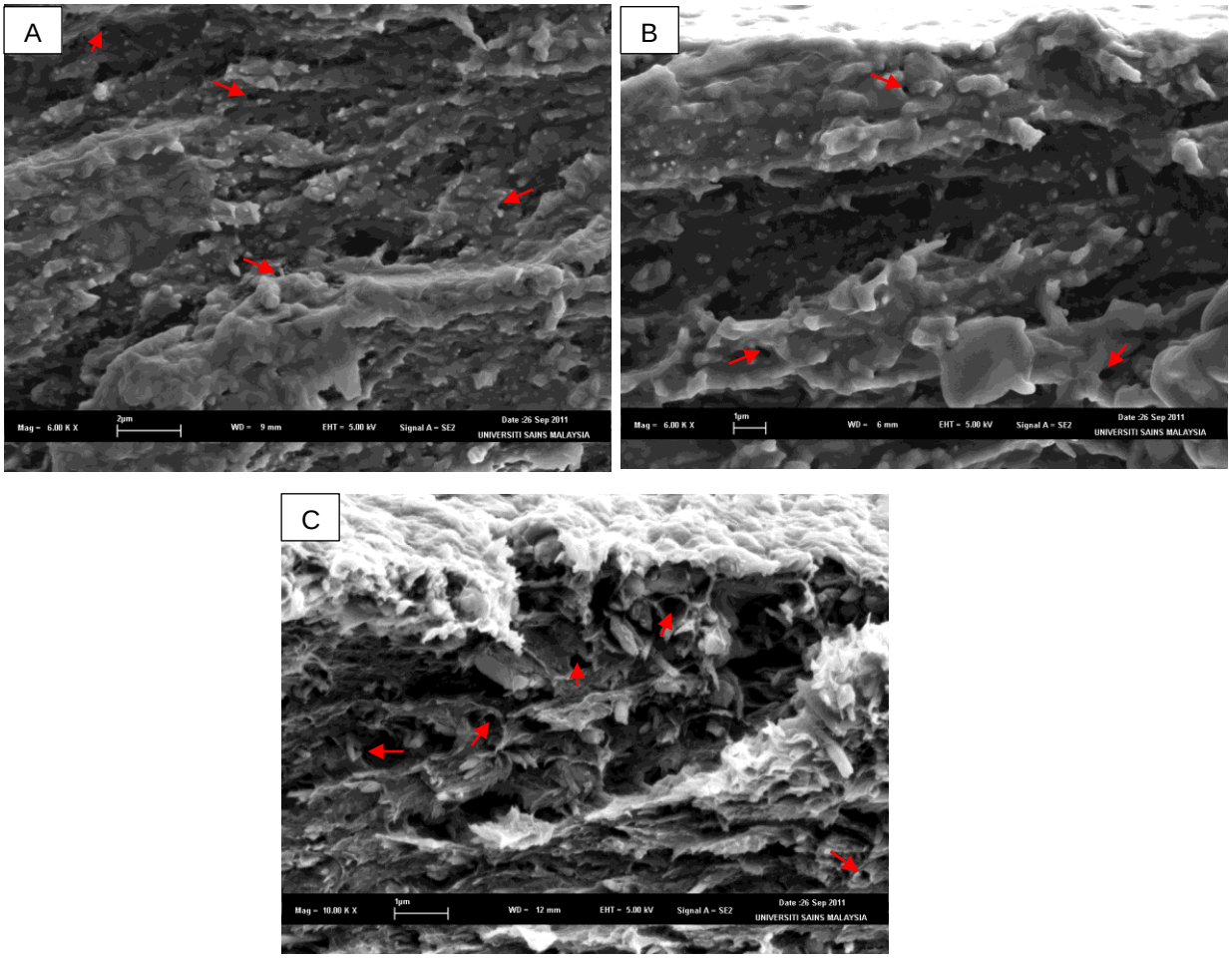

Figure 1: SEM images of CS membranes with (A) 2(w/w %) (B) 5(w/w %) and (C) 15 (w/w %) of HNTs.

3.3 FTIR Analysis

According to FTIR spectra for pure chitosan, pure HNT, and chitosan membranes with 0, 5 and 15 (w/w %) HNTs the presence of functional groups of chitosan and HNTs can be identified in the composite membranes. The main functional groups that appeared in the chitosan spectrum were vibration of OH groups at 3353 cm^{-1} and 3297 cm^{-1}, C-H bond ($-CH_3$) at 2873 cm^{-1}, carbonyl bonds (C=O) of amide groups C=O-NHR at 1680-1480 cm^{-1}, bending vibration of methylene groups at 1375 cm^{-1} and asymmetric vibration of CO at 1150 cm^{-1} [9, 15], have also appeared in the chitosan membranes, with 0, 5 and 15 (w/w %) HNTs concentrations. This indicated that functional groups of chitosan have been repeated in the membranes as well.

For the pure HNT, the main bands appearing in the spectrum included; O-H deformation of inner hydroxyl groups at 911 cm^{-1}, in-plane Si-O stretching at 1031m^{-1}, O-H stretching of

inner hydroxyl groups at 3621 cm^{-1} and O-H stretching of inner – surface hydroxyl groups at 3695 cm^{-1} [16], have also appeared in the chitosan membranes with 5 and 15 (w/w %) HNT concentration.

The peak appeared at 1117.88 cm^{-1} in the pure HNT spectrum corresponded to perpendicular Si-O stretching, has also appeared in the 15 (w/w %) HNT loaded membrane, but not in the other membranes. This finding implied that at High HNT concentration HNTs have not reacted with chitosan uniformly due to the formation of HNT agglomerated particles.

By increasing the HNT concentration to 5 and 15 (w/w %), the intensity of the band at 1030 cm^{-1}(external surface siloxane groups) decreased significantly. Even though the intensity has decreased with increasing the HNT concentration, it remained constant for 5 and 15 (w/w %) HNT loaded membranes. This consistency implied that the external surface siloxane groups (Si-O) (v = 1030 cm^{-1}) of HNTs have chemically interacted with the matrix (chitosan) up to its' maximum extent and are not reacting further with the addition of HNTs. The functional groups (COH, COC and CH_2OH) corresponding to the peak at 1063 cm^{-1} in pure chitosan can be seen in the 0 w% HNT membrane (control sample), but the peak has disappeared in 5 and 15 (w/w %) HNT membranes. This suggested that these functional groups have reacted with some other functional groups in HNTs.

Moreover, the amide I bands for chitosan membranes for 5and 15 (w/w %) have slightly shifted towards low wavelengths values. The amide I band for pure chitosan and chitosan membranes was at 1653 cm^{-1} for the 0 (w/w %) HNTs, 1647 cm^{-1} for the 5 (w/w %) HNTs, and 1650 $cm^{-}1$ for the 15 (w/w %) HNTs. Theoretically, amide bands shifting to low wave lengths indicated the occurrence of hydrogen-bonding between the chitosan and fillers [1]. In this case, the amide I band of chitosan membranes with 5 (w/w %) HNTs shifted more towards the low wavelengths than the 15 (w/w %) HNTs loaded chitosan membranes. This result indicated a possible formation of hydrogen-bonding between chitosan and HNT in nanocomposite membranes.

3.4 Thermogravimetric Analysis (TGA)

TGA curves are summarized in Table 2. As far as 50% and maximum weight loss was concerned, it can be observed that the corresponding temperatures of chitosan membranes with 2, 10 and 15 (w/w %) of HNTs have drastically increased; especially at 50% weight loss.

Enhancement of thermal stability could occur due to two main reasons. Char residue contributed to enhance the thermal stability of a composite. Char formation occurred at the expense of volatiles and the char itself acted as a barrier and hinder the diffusion of volatile loss. Hence, char residue of chitosan/HNT nanocomposites may act as a barrier and hinder the volatile escape while helping to improve the thermal stability. As mentioned by Du et al. (2006), the lumens of HNTs contributed to enhance the thermal stability of the polymer/HNT nanocomposite. In general, the length of HNTs varies from 50 to 5000 nm, with an external diameter of 20-200nm and internal diameter of 10-70nm. Therefore, the HNTs' lumen may have high volume percentage (between 10 to 30%) [11]. During the initial degradation stage of the membranes, degraded products of chitosan may be considerably entrapped within the

lumens of HNTs. Hence, it may have led to effective delay in mass transport and therefore, thermal stability has significantly increased at high concentrations.

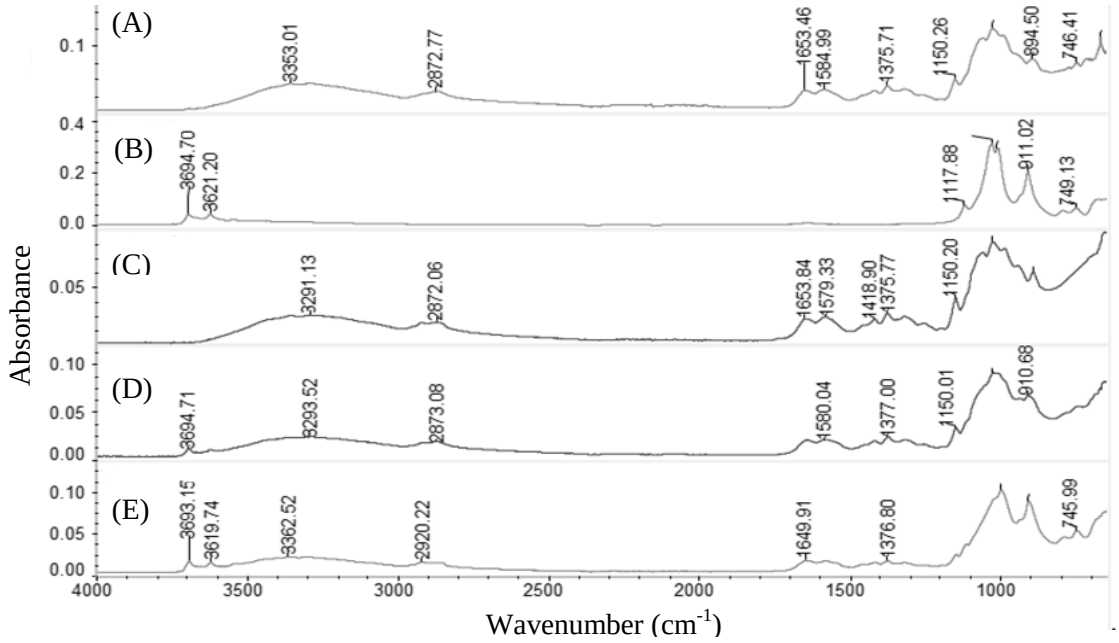

Figure 2: FTIR spectra of (a) Pure chitosan, (b) Pure HNT, (C) chitosan membrane with 0 w% HNTs, (d) chitosan membrane with 5 w% HNTs and (e) chitosan membrane with 15 w% HNTs.

HNT composition (w/w %)	Temperature at 5% weight loss (°C)	Temperature at 50% weight loss (°C)	Maximum weight loss (%)	Temperature at maximum weight (loss rate/°C)
0	45	370	35	295
2	50	375	38	302
5	45	380	37	300
10	50	396	39	301
15	45	455	44	297
Pure HNT	450	498	-	85

Table 2: Summary of the TGA results for CS and its composites.

4.0 Conclusion

Tensile measurements, SEM micrographs, TGA and FTIR analysis confirmed that Chitosan/HNT membranes were prepared successfully by using solution casting method after adding 2, 5, 10 and 15 (w/w %) of natural halloysite nanotubes. With the incorporation of 5(w/w %) of HNTs, the mechanical properties, such as the Young's modulus and tensile strength of the nanocomposites, significantly improved by 21% and 34%, respectively however at high concentrations HNT agglomeration and less filler-matrix interaction were the major reasons for slightly reduction in tensile properties of the membranes.

Acknowledgements

This work is funded by a Fundamental Research Grant Scheme (FRGS) grant FRGS2/2010/SG/MUSM/02/6) from the Ministry of Higher Education, Malaysia.

References

[1] Tang C., Chen N., Zhang Q., Wang K., Fu Q., Zhang X., Preparation and properties of chitosan nanocomposites with nanofillers of different dimensions. *Polymer Degradation and Stability,* **vol. 94**, pp. 124-131 (2009).

[2] Hong S.I., Lee J.H., Bae H.J., Koo S.Y., Lee H.S., Choi J.H., Kim D.H., Park S.H., Park H.J. Effect of shear rate on structural, mechanical, and barrier properties of chitosan/montmorillonite nanocomposite film. *Journal of Applied Polymer Science,* **vol. 119**, pp. 2742-2749 (2011).

[3] Wang S., Chen L., Tong Y. Structure-property relationship in chitosan-based biopolymer/montmorillonite nanocomposites. *Journal of Polymer Science Part A: Polymer Chemistry,* **vol. 44**, pp. 686-696 (2006).

[4] Jayakumar R., Prabaharan M., Kumar P.T., Nair S.V., Tamura H. Biomaterials based on chitin and chitosan in wound dressing applications. *Biotechnology Advances,* **vol. 29**, pp. 322-337 (2011).

[5] Venkatesan J., Kim S.K. Chitosan composites for bone tissue engineering – An Overview. *Marine Drugs,* **vol. 8**, pp. 2252-2266 (2010).

[6] De Brum, O.G., Maggioni J.F., Nunes A. Chitosan membranes for pressure filteration. *Journal of the Brazilian Chemical Society,* **vol. 6**, pp. 353-356 (1995).

[7] Tang L.X.C., Su J., Wang K., Yang C., Zhang Q., Fu Q. Largely improved tensile properties of chitosan film via unique synergistic reinforcing effect of carbon nanotube and clay. *Journal of Physical Chemistry,* **Vol. 112**, pp. 3876-3881 (2008).

[8] Feng Wang L.S.S., De Zhang W., Tong Y. J. Preparation and mechanical properties of chitosan/carbon nanotubes composites. *Biomacromolecules,* **vol. 6**, pp. 3067-3072 (2005).

[9] Paluszkiewicz C., Stodolak E., Hasik M., Blazewicz M. FT-IR study of montmorillonite–chitosan nanocomposite materials. *Spectrochimica Acta Part A: Molecular and Biomolecular Spectroscopy,* **vol. 79**, pp. 784-788 (2011).

[10] Xie Y., Chang P.R., Wang S., Yu J., Ma X. Preparation and properties of halloysite nanotubes/plasticized Dioscorea opposita Thunb. starch composites. *Carbohydrate Polymers*, **vol. 83**, pp. 186-191 (2011).

[11] Keeling J., Pasbakhsh P., Churchman G.J. *Halloysite from the Eucla Basin, South Australia-Comparison of physical properties for potential new uses* in "Proceeding of *10th International Congress for Applied Mineralogy (ICAM)*", Trondheim, Norway, (2011).

[12] Pasbakhsh P., Ismail H., Fauzi M.N.A., Bakar A.A. EPDM/ modified halloysite nanocomposites. *Applied Clay Science,* **vol. 48**, pp. 405-413 (2010).

[13] Dobrovol'skaya I.P., Popryadukhin P.V., Khomenko A.Y., Dresvyanina E.N., Yudin V.E., Elokhovskii V.Y., Chvalun S.N., Saprykina N.N., Maslennikova T.P., Korytkova E.N., Structure and characteristics of chitosan-based fibers containing chrysotile and halloysite. *Polymer Science Series A,* **vol. 53**, pp. 418-423 (2011).

[14] Fu S.Y., Feng X.Q., Lauke B., Mai Y.W. Effects of particle size, particle/matrix interface adhesion and particle loading on mechanical properties of particulate-polymer composites. *Composites Part B: Engineering,* **vol. 39**, pp. 933-961 (2008).

[15] Basal G., Sirin Deveci S.,Yalcin D., Bayraktar O. Properties of n-eicosane-loaded silk fibroin-chitosan microcapsules. *Journal of Applied Polymer Science,* **vol. 121**, pp. 1885-1889 (2011).

[16] Yuan P., Southon P.D., Liu Z., Green M.E.R., Hook J.M., Antill S.J., Kepert C.J. Functionalization of halloysite clay nanotubes by grafting with γ-Aminopropyltriethoxysilane. *Journal of Physical Chemistry C,* **vol. 112**, pp. 15742-1575 (2008).